

BlackIoT: IoT Botnet of High Wattage Devices Can Disrupt the Power Grid

Saleh Soltan

*Department of Electrical Engineering
Princeton University
ssoltan@princeton.edu*

Prateek Mittal

*Department of Electrical Engineering
Princeton University
pmittal@princeton.edu*

H. Vincent Poor

*Department of Electrical Engineering
Princeton University
poor@princeton.edu*

Abstract

We demonstrate that an Internet of Things (IoT) botnet of high wattage devices—such as air conditioners and heaters—gives a unique ability to adversaries to launch large-scale coordinated attacks on the power grid. In particular, we reveal a new class of potential attacks on power grids called the Manipulation of demand via IoT (MadIoT) attacks that can leverage such a botnet in order to manipulate the power demand in the grid. We study five variations of the MadIoT attacks and evaluate their effectiveness via state-of-the-art simulators on real-world power grid models. These simulation results demonstrate that the MadIoT attacks can result in local power outages and in the worst cases, large-scale blackouts. Moreover, we show that these attacks can rather be used to increase the operating cost of the grid to benefit a few utilities in the electricity market. This work sheds light upon the interdependency between the vulnerability of the IoT and that of the other networks such as the power grid whose security requires attention from both the systems security and power engineering communities.

1 Introduction

A number of recent studies have revealed the vulnerabilities of the Internet of Things (IoT) to intruders [21, 49, 50]. These studies demonstrated that IoT devices from cameras to locks can be compromised either directly or through their designated mobile applications by an adversary [12, 28, 43]. However, most previous work has focused on the consequences of these vulnerabilities on personal privacy and security. It was not until recently and in the aftermath of the Distributed Denial of Service (DDoS) attack by the Mirai botnet, comprising six hundred thousand compromised devices targeting victim servers, that the collective effect of the IoT vulnerabilities was demonstrated [12]. In this paper, we reveal another substantial way that compromised IoT devices can be utilized by an adversary to disrupt one of the

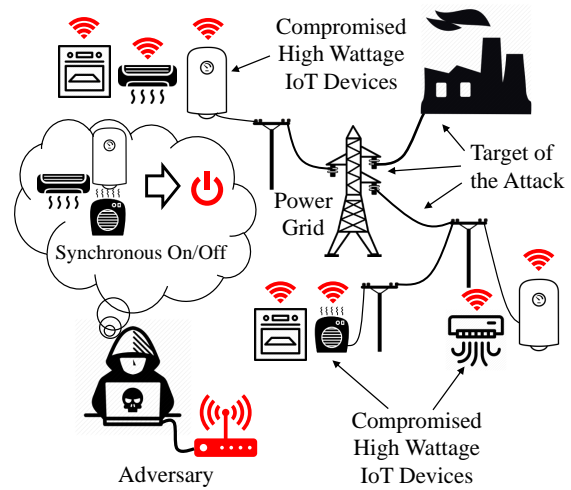


Figure 1: The MadIoT attack. An adversary can disrupt the power grid’s normal operation by synchronously switching on/off compromised high wattage IoT devices.

most essential modern infrastructure networks, the power grid.

Power grid security standards are all based on the assumption that the power demand can be predicted reliably on an hourly and daily basis [62]. Power grid operators typically assume that power consumers collectively behave similarly to how they did in the past and under similar conditions (e.g., time of the day, season, and weather). However, with the ubiquity of IoT devices and their poor security measures (as shown in [12]), we demonstrate that this is no longer a safe assumption.

There has been a recent trend in producing Wi-Fi enabled high wattage appliances such as air conditioners, water heaters, ovens, and space heaters that can now be controlled remotely and via the Internet [3] (for the power consumption of these devices see Table 1). Even older appliances can be remotely controlled by adding Wi-Fi enabled peripherals such as Tado° [8] and Aquanta [2]. A group of these devices can also be controlled remotely or automatically using smart thermostats or home assistants

such as Amazon Echo [1] or Google Home [4]. Hence, once compromised, any of these devices can be used to control high wattage appliances remotely by an adversary to manipulate the power demand.

In this paper, we reveal a new class of potential attacks called the Manipulation of demand via IoT (MadIoT) attacks that *allow an adversary to disrupt the power grid’s normal operation by manipulating the total power demand using compromised IoT devices* (see Fig. 1). These attacks, in the extreme case, can cause large scale blackouts. An important characteristic of MadIoT attacks is that unlike most of previous attacks on the power grid, they do not target the power grid’s Supervisory Control And Data Acquisitions (SCADA) system but rather the loads that are much less protected as in load-altering attacks studied in [11, 41].

It is a common belief that manipulating the power demands can potentially damage the power grid. However, these speculations have mostly remained unexamined until our work. *We are among the first to reveal realistic mechanisms to cause abrupt distributed power demand changes using IoT devices—along with Dvorkin and Sang [24], and Dabrowski et al. [19]. Our key contribution is to rigorously study the effects of such attacks on the power grid from novel operational perspectives (for more details on the related work see Section 6).*

We study five variations of the MadIoT attacks and demonstrate their effectiveness on the operation of real-world power grid models via state-of-the-art simulators. These attacks can be categorized into three types:

(i) Attacks that result in frequency instability:

An abrupt increase (similarly decrease) in the power demands—*potentially by synchronously switching on or off many high wattage IoT devices*—results in an imbalance between the supply and demand. This imbalance instantly results in a sudden drop in the system’s frequency. If the imbalance is greater than the system’s threshold, the frequency may reach a critical value that causes generators tripping and potentially a large-scale blackout. For example, using state-of-the-art simulators on the small-scale power grid model of the Western System Coordinating Council (WSCC), we show that a *30% increase in the demand results in tripping of all the generators. For such an attack, an adversary requires access to about 90 thousand air conditioners or 18 thousand electric water heaters within the targeted geographical area.* We also study the effect of such an attack during the system’s restarting process after a blackout (a.k.a. the *black start*) and show that it can disrupt this process by causing frequency instability in the system.

(ii) Attacks that cause line failures and result in cascading failures: If the imbalance in the supply and demand after the attack is not significant, the frequency of

Table 1: Home appliances’ approximate electric power usage based on appliances manufactured by General Electric [3].

Appliance	Power Usage (W)
Air Conditioner	1,000
Space Heater	1,500
Air Purifier	200
Electric Water Heater	5,000
Electric Oven	4,000

the system is stabilized by the *primary controller* of the generators. Since the way power is transmitted in the power grid (a.k.a. the *power flows*) follows Kirchhoff’s laws, the grid operator has almost no control over the power flows after the response of the primary controllers. Hence, even a small increase in the demands may result in line overloads and failures. These initial line failures may consequently result in further line failures or as it is called, a *cascading failure* [54]. For example, we show by simulations that *an increase of only 1% in the demand in the Polish grid during the Summer 2008 peak, results in a cascading failure with 263 line failures and outage in 86% of the loads. Such an attack by the adversary requires access to about 210 thousand air conditioners which is 1.5% of the total number of households in Poland [58].* During the Summer peak hours when most of the air conditioners are already on, decreasing their temperature set points [61] combined with the initiation of other high wattage appliances like water heaters, can result in the same total amount of increase in the demand.

We also show that an adversary can cause line failures by *redistributing the demand* via increasing the demand in some places (e.g., turning on appliances within a certain IP range) and decreasing the demand in others (e.g., turning off appliances within another IP range). These attacks, in particular, can cause failures in important high capacity *tie-lines* that connect two neighboring independent power systems—e.g., of neighboring countries.

(iii) Attacks that increase operating costs: When the demand goes above the day-ahead predicted value, conservatively assuming that there would be no frequency disturbances or line failures, the grid operator needs to purchase additional electric power from ancillary services (i.e., reserve generators). These reserve generators usually have higher prices than the generators committed as part of day ahead planning. Therefore, using the reserve generators can significantly increase the power generation cost for the grid operator but at the same time be profitable for the utility that operates the reserve generators. For example, we show by simulations that *a 5% increase in the power demand during peak hours by an adversary can result in a 20% increase in the power generation cost.* Hence, an adversary’s attack may rather be for the benefit of a particular utility in the electricity market than for damaging the infrastructure.

The MadIoT attacks’ sources are *hard to detect and disconnect* by the grid operator due to their distributed nature. These attacks can be *easily repeated* until being effective and are *black-box* since the attacker does not need to know the operational details of the power grid. These properties make countering the MadIoT attacks challenging. Nevertheless, we provide sketches of countermeasures against the MadIoT attacks from both the power grid and the IoT perspectives.

Overall, our work sheds light upon the interdependency between the vulnerability of the IoT and that of other networks such as the power grid whose security requires attention from both the systems security and the power engineering communities. We hope that our work serves to protect the grid against future threats from insecure IoT devices.

The rest of this paper is organized as follows. Section 2 provides a brief introduction to power systems. In Section 3, we introduce the MadIoT attack and its variations, and in Section 4, we demonstrate these attacks via simulations. In Section 5, we present countermeasure sketches against the MadIoT attacks. Section 6 presents a summary of the related work, and Section 7 discusses the limitations of our work. Finally Section 8 provides concluding remarks and recommendations. The central results of the paper are self-contained in the above sections. We refer the interested reader to the appendix for an overview of recent blackouts and their connection to MadIoT attacks, and additional experimental results.

2 Power Systems Background

In this section, we provide a brief introduction to power systems. For more details, refer to [26, 27, 31, 62].

2.1 Basics

Power systems consist of different components (see Fig. 2). The electric power is generated at power generators at different locations with different capacities and then transmitted via a high voltage *transmission network* to large industrial consumers or to the lower voltage *distribution network* of a town or a city. The power is then transmitted to commercial and residential consumers.

The main challenges in the operation and control of the power systems are in the transmission network. Moreover, since a distributed increase in power demand does not significantly affect the operation of the distribution network, we ignore the operational details of the distribution network and only consider it as an aggregated load within the transmission network. The term *power grid* mainly refers to the transmission network rather than the distribution network.

The transmission network can have a very complex topology. Each intersection point in the grid is called a

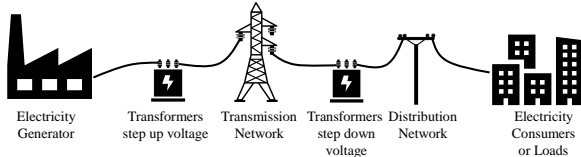


Figure 2: Main components of a power system.

bus which is a node in the equivalent graph.¹ Some of the buses may be connected to the distribution network of a city or a town and therefore represent the aggregated load within those places.

The instantaneous electric power generation and consumption are measured in watts (W) and are calculated based on electric voltages and currents. Almost all the power systems deploy Alternating Currents (AC) and voltages for transmitting electric power. This means that the electric current and voltage at each location and each point in time are equal to $I(t) = \sqrt{2}I_{\text{rms}} \cos(2\pi ft + \theta_I)$ and $V(t) = \sqrt{2}V_{\text{rms}} \cos(2\pi ft + \theta_V)$, in which f is the *nominal frequency* of the system, and $I_{\text{rms}}, V_{\text{rms}}$ and θ_I, θ_V are the root mean square (rms) values and the phase angles of the currents and voltages, respectively. In the U.S., Canada, Brazil, and Japan the power system frequency is 60Hz but almost everywhere else it is 50Hz .

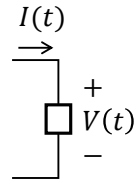


Figure 3

Given the voltages and the currents, the *active, reactive, and apparent power* amplitudes absorbed by a load can be computed as $P = V_{\text{rms}}I_{\text{rms}} \cos(\theta_V - \theta_I)$, $Q = V_{\text{rms}}I_{\text{rms}} \sin(\theta_V - \theta_I)$, and $S = V_{\text{rms}}I_{\text{rms}}$, respectively. $\cos(\theta_V - \theta_I)$ is called the *power factor* of a load.

2.2 Power Grid Operation and Control

Stable operation of the power grid relies on the persistent balance between the power supply and the demand. This is mainly due to the lack of practical large scale electrical power storage. In order to keep the balance between the power supply and the demand, power system operators use weather data as well as historical power consumption data to predict the power demand on a daily and hourly basis [27]. This allows the system operators to plan in advance and only deploy enough generators to meet the demand in the hours ahead without overloading any power lines. The grid operation should also comply with the *$N - 1$ security standard*. The $N - 1$ standard requires the grid to operate normally even after a failure in a *single* component of the grid (e.g., a generator, a line, or a transformer).

In power systems, the rotating speed of generators cor-

¹The terms “bus” and “node” can be used interchangeably in this paper without loss of any critical information.

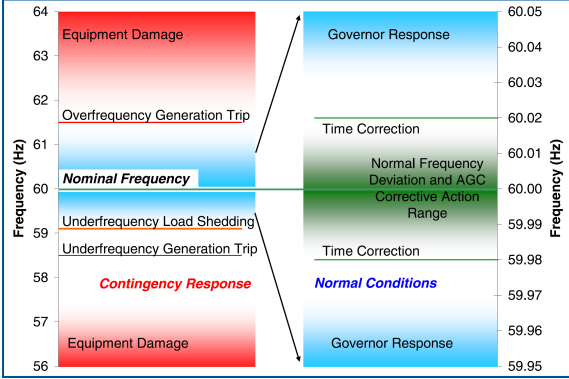


Figure 4: Normal and abnormal frequency ranges in North America. The figure is borrowed from [60].

respond to the frequency. When the demand gets greater than the supply, the rotating speeds of the turbine generators' rotors decelerate, and the kinetic energy of the rotors are released into the system in response to the extra demand. Correspondingly, this causes a drop in the system's frequency. This behavior of turbine generators corresponds to Newton's first law of motion and is calculated by the *inertia* of the generator. Similarly, the supply being greater than the demand results in acceleration of the generators' rotors and a rise in the system's frequency.

This decrease/increase in the frequency of the system cannot be tolerated for a long time since frequencies lower than the nominal value severely damage the generators. If the frequency goes above or below a threshold value, protection relays turn off or disconnect the generators completely (see Fig. 4 for normal and abnormal frequency ranges in North America). Hence, within seconds of the first signs of decrease in the frequency, the *primary controller* activates and increases the mechanical input which increases the speed of the generator's rotor and correspondingly the frequency of the system [26].

Despite stability of the system's frequency after the primary controller's response, it may not return to its nominal frequency (mainly due to the generators generating more than their nominal value). Hence, the *secondary controller* starts within minutes to restore the system's frequency. The secondary controller modifies the active power set points and deploys available extra generators and controllable demands to restore the nominal frequency and permanently stabilizes the system.

2.3 Power Flows

The equality of supply and demand is a necessary condition for the stable operation of the grid, but it is far from being sufficient. In order to deliver power from generators to loads, the electric power should be transmitted by the transmission lines. The power transmitted on each line is known as the *power flow* on that line.

Unlike routing in computer networks, power flows are

almost entirely determined and governed by Kirchhoff's laws given the active and reactive power demand and supply values. Besides the constraints on the power flows enforced by Kirchhoff's laws, there are other limiting constraints that are dictated by the physical properties of the electrical equipment. In particular, each power line has a certain capacity of apparent power that it can carry safely.

Unlike water or gas pipelines, the capacity constraint on a power line is not automatically enforced by its physical properties. Once the power supply and demand values are set, the power flows on the lines are determined based on Kirchhoff's laws with no capacity constraints in the equations. Thus, an unpredicted supply and demand setting may result in electric power *overload* on some of the lines. Once a line is overloaded, it may be *tripped* by the protective relay, or it may break due to overheating—which should be avoided by the relay. Hence, the system operator needs to compute the power flows in advance—using the predicted demand values and optimal set of generators to supply the demand—to see if any of the lines will be overloaded. If so, the configuration of the generators should be changed to avoid lines overload and tripping.

2.4 Voltage Stability

Besides power line thermal limits, the power flows on the lines are limited by their terminating buses' voltages. The voltages at the buses are controlled by maintaining the level of the reactive power (Q) supply. Voltage instability or as it is called *voltage collapse* occurs when the generated reactive power becomes inadequate. This is mainly due to changes in system configurations due to line failures, increase in active or reactive power demand, or loss of generators. Voltage collapse should be studied using $V-Q$ (characterizing the relationship between the voltage at the terminating bus of a line to the reactive power flow) and $P-V$ (characterizing the relationship between the voltage at the terminating bus of a line to the active power flow) analysis which is beyond the scope of this paper, but for more details see [62, Chapter 7].

Voltage collapse results in the infeasibility of the power flow equations. Hence, it can be detected when the power flow solver fails to find a solution to the power flow equation (usually after an initial change in the system). In such scenarios, the grid operator is forced to perform load shedding (i.e., outage in part of the grid) in order to recover the system from a voltage collapse and make the power flow equations feasible again. Hence, even failures in a few lines or an increase in the active/reactive power demands may result in large scale outages around the grid due to voltage collapse.

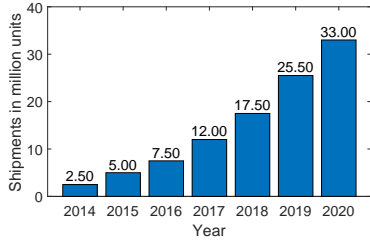


Figure 5: Estimated number of homes with smart thermostats in North America in millions. Data is obtained from Statista [56].

3 Attacking the Grid Using an IoT Botnet

In this section, we reveal attack mechanisms that can utilize an IoT botnet of high wattage devices to launch a large-scale coordinated attack on the power grid.

3.1 Threat Model

We assume that an adversary has already gained access to an IoT botnet of many high wattage smart appliances (listed in Table 1) within a city, a country, or a continent. Since most of the IoT devices are controlled using mobile phone applications, access to users’ mobile phones or corresponding applications can also be used to control these devices [28]. This access can potentially allow the adversary to increase or decrease the demand in different locations remotely and synchronously. The adversary’s power to manipulate the demand can also be translated into watts (W) using the numbers in Table 1 and based on the type and the number of devices to which it has access.

For example, if we consider only the houses with smart thermostats in 2018 as shown in Fig. 5 and assuming that each thermostat only controls two $1kW$ air conditioners, an attacker can *potentially* control $35GW$ of electric power²—even a fraction of which is a significant amount. Recall that in the case of the Mirai botnet, the attackers could get access to about 600 thousand devices within a few months [12].

The $35GW$ is computed by only considering the thermostats connected to a few air conditioners. By considering all the smart air conditioners as well as other high wattage appliances such as water heaters, this value would be much higher. Moreover, this amount will grow in the future as the trend shows in Fig. 5.

We call the attacks under this threat model the Manipulation of the demand via IoT (MadIoT) attacks. In the next subsection, we provide the details of various types of attacks that can be performed by an adversary.

3.2 MadIoT Attack Variations

MadIoT attacks can disrupt the normal operation of the power grid in many ways. Here, we present the most im-

²For the sake of comparison, this amount is equal to 7% of the entire U.S. 2017 Winter peak demand (about $500GW$) [10].

portant and direct ways that such attacks can cause damage to the grid (summarized in Table 2):

1. Significant frequency drop/rise: As briefly described in Section 2, the normal operation of the power grid relies on the persistent balance between the supply and demand. Thus, an adversary’s approach could be to disrupt this balance using an IoT botnet. An adversary can leverage an IoT botnet of high-wattage devices and synchronously switch on all the compromised devices. *If the resulting sudden increase in the demand is greater than a threshold, which depends on the inertia of the system, it can cause the system’s frequency to drop significantly before the primary controllers can react. This consequently may result in the activation of the generators’ protective relays and loss of generators, and finally a blackout.* Sudden decrease in the demand may also result in the same effect but this time by causing a sudden rise in the frequency.

An adversary can further increase its success by strategic selection of the timing of an attack using the online data available via the websites of Independent System Operators (ISOs)³ (e.g., daily fuel mix and live updates of the demand values.) For example, we know that as the share of renewable resources in the power generation increases, the inertia of the system decreases. Therefore, an attack that is coordinated with the time that renewable penetration is highest, is more effective in causing large changes in the frequency. Similarly, an attack during the peak hours can result in a slow yet persistent frequency drop in the system. Such an attack may exhaust the controller reserves and force the system operator to perform load shedding. This may result in power outages in several parts of the system if the situation is handled well by the operator, or in a large-scale blackout if it is mishandled and the system’s frequency keeps dropping. According to the European Network of Transmission System Operators for Electricity (ENTSOE) guidelines, if the frequency of the European grid goes below $47.5Hz$ or above $51.5Hz$, a blackout can hardly be avoided [25].

2. Disrupting a black start: Once there is a blackout, the grid operator needs to restart the system as soon as possible. This process is called a *black start*. Since the demand is unknown at the time of a black start, restarting the whole grid at the same time may result in frequency instability and system failure again. Hence, in a black start, the operator divides the system into smaller *islands* and tries to restart the grid in each island separately. The islands are then connected to increase the reliability of the system.

Since the grid is partitioned into smaller islands at

³The system operators are given different names in different countries and continents, but here for the sake of simplicity, we refer to all of them as ISOs.

Table 2: MadIoT attack variations. The botnet size is in bots/ MW which is the number of bots required to perform a successful variation of the MadIoT attack, if the total demand in the system is $1MW$. All the bots are assumed to be air conditioners.

#	Goal	Attack action	Initial impact	Botnet size	Simulation results
1	Grid frequency rise/drop	Synchronously switching on/off all the bots	Generation tripping	200–300	Figs. 8,7,9
2	Disrupting grid re-start	Synchronously switching on all the bots once the power restarts after a blackout	Generation tripping	100–200	Fig. 11
3	Line failures and cascades	Synchronously switching on or off the bots in different locations	Lines tripping	4–10	Figs. 12,13,15
4	Failure in tie-lines	Synchronously switching on (off) the bots in importing (exporting) end of a tie-line	Tie-lines tripping	10–15	Fig. 16
5	Increasing the operating cost	Slowly switching on the bots during power demand peak hours	Utilizing power generation reserve	30–50	Fig. 17

the time of a black start, the inertia of each part is low and therefore the system is very vulnerable to demand changes. Thus, an adversary can significantly hinder the black start process by suddenly increasing the demand using the IoT botnet once an island is up. This can cause a large frequency disturbance in each island and cause the grid to return to the blackout state.

3. Line failures and cascades: Recall from Section 2.3 that the power flows in power grids are determined by the Kirchhoff’s laws. Therefore, most of the time, the grid operator does not have any control over the power flows from generators to loads. Once an adversary causes a sudden increase in the loads all around the grid, assuming that the frequency drop is not significant, the extra demand is satisfied by the primary controller. Since the power flows are not controlled by the grid operator at this stage, this may result in line overloads and consequent lines tripping.

After initial lines tripping or failures, the power flows carried by these lines are redistributed to other lines based on Kirchhoff’s laws. Therefore, the initial line failures may subsequently result in further line failures or, as it is called, a *cascading failure* [54]. These failures may eventually result in the separation of the system into smaller unbalanced islands and a large-scale blackout.

Moreover, failure in a few lines accompanied by an increase in the power demand may result in a voltage collapse (recall from Section 2.4) which consequently would force the grid operator to perform load shedding. Hence, in some steps during the cascade, there are more outages due to load shedding.

An adversary may also start cascading line failures by redistributing the loads in the system by increasing the demand in a few locations and decreasing the demand in others in order to keep the total demand constant. This redistribution of the demand in the system may result in line failures without causing any frequency disturbances. The advantage of this attack is that it may have the same effect without attracting a lot of attention from the grid operator. It can be considered to be a *stealthier* version

of the *demand increase only* attack.

4. Failures in the tie-lines: Tie-lines between the ISOs are among the most important lines within an interconnection. These tie-lines are usually used for carrying large amounts of power as part of an exchange program between two ISOs. Failure in one of these lines may result in a huge power deficit (usually more than $1GW$) in the receiving ISO and most likely a blackout due to the subsequent frequency disturbances or a large-scale outage due to load shedding by the grid operator.

Due to their importance, the tie-lines can be the target of an adversary. An adversary can observe the actual power flows on the tie-lines through ISOs’ websites, and target the one that is carrying power flow near its capacity. In order to overload that line, all the adversary needs to do is to turn on the high wattage IoT devices in the area at the importing end of the line and turn off the ones at the exporting end (using the IP addresses of the devices).⁴ This can overload the tie-line and cause it to trip by triggering its protective relay.

5. Increasing the operating cost: When the demand goes above the predicted value, the ISO needs to purchase additional electric power from ancillary services (i.e., reserve generators). These reserve generators usually have a higher price than the generators committed as part of the day ahead planning. Thus, using the reserve generators can significantly increase the power generation cost for the grid operator but at the same time be profitable for the utility that operates the reserve generator.

Hence, the goal of an adversary’s attack may be to benefit a particular utility in the electricity market rather than to damage the infrastructure. The adversary can achieve this goal by slowly increasing the demand (e.g., switching on a few devices at a time) at a particular time of the day and in a certain location. Moreover, it may reach out

⁴A sudden increase in the demand, only at the importing end of the tie-line, may also result in its overload. This is due to the fact that once there is an imbalance between the supply and demand, all the generators within an interconnection (whether inside or outside of the particular ISO) respond to the imbalance which consequently results in an increase in the power flow on the tie-line.

to utilities to act in their favor in return for a payment.

Overall, the above attacks demonstrate that *an adversary as described in Section 3.1 has tremendous power to manipulate the operation of the grid in many ways which were not possible a few years ago in the absence of IoT devices.*

3.3 Properties and Defensive Challenges

The MadIoT attacks have unique properties that make them very effective and at the same time very hard to defend against. In this subsection, we briefly describe some of these properties.

First, the sources of the MadIoT attacks are *very hard to detect and disconnect* by the grid operator. The main reason is that the security breach is in the IoT devices, yet the attack is on the power grid. The grid operator cannot easily detect which houses are affected since it only sees the aggregation of the distributed changes in the demand around the grid. At the same time, the attack does not noticeably affect the performance of the IoT devices, especially if the smart thermostat is attacked. Moreover, the attack may not be noticeable by the households since the changes are temporary and can be considered as part of the automatic temperature control.

Second, the MadIoT attacks are *easy to repeat*. An adversary can easily repeat an attack at different times of the day and different days to find a time when the attack is the most effective. Moreover, this repeatability allows an adversary to cause a *persistent blackout* in the power grid by disrupting the black start process as described in the previous subsection.

Third, the MadIoT attacks are *black-box*. An adversary does not need to know the underlying topology or the detailed operational properties of the grid, albeit it can use the high-level information available on the ISOs' websites to improve the timing of its attack. It can also use the repeatability of these attacks and general properties of the power grids to achieve and perform a successful attack.

Finally, *power grids are not prepared to defend against the MadIoT attacks*, since abrupt changes in the demand are not part of the *contingency list* that grid operators are prepared for. As mentioned in Section 2, power grids are required to operate normally after a failure in a single component of the grid (the $N - 1$ standard). Therefore, the daily operation of the grid is planned such that even a failure in the largest generator does not affect its normal operation.

The scenarios predicted by the $N - 1$ standard, however, are quite different from the scenarios caused by the MadIoT attacks. Although an increase in the demand can be similar to losing a generator from the supply and demand balance perspective, these two phenomena result

in completely different power flows in the grid. Hence, although losing a generator may not result in any issues as planned, increase in the demands by an adversary may result in many line overloads. Moreover, *the imbalance caused by an adversary may surpass the imbalance caused due to losing the largest generator*, and therefore results in unpredicted frequency disturbances. For example, the capacity of the largest operating generator in the system may be $1GW$ (usually a nuclear power plant) which can be surpassed by an attack comprising more than 100 thousand compromised water heaters.

Despite these difficulties, we provide sketches of countermeasures against the MadIoT attacks in Section 5.

3.4 Connection to Historical Blackouts

There have been several large-scale blackouts in the past two decades around the world. Although these events were not caused by any attacks, the chain of events that led to these blackouts could have been initiated by a MadIoT attack. For example, the initial reactive power deficit in Ohio in 2003 leading to the large-scale blackout in the U.S. and Canada [60], and the failures in the tie-lines connecting Italy to Switzerland in 2003 leading to the complete shutdown of the Italian grid [59], could have been caused by MadIoT attacks. Most of these events happened because the systems' operators were *not prepared for the unexpected initial event*. Hence, the MadIoT attacks could result in similar unexpected failures. We reviewed a few of the recent blackouts in the power grids around the world and demonstrated how an adversary could have caused similar blackouts. The details of these events are relegated to Appendix A.

4 Experimental Demonstrations

In this section, we demonstrate the effectiveness of the MadIoT attacks on real-world power grid models via state-of-the-art simulators. Recall that the MadIoT attacks are black-box. Therefore, *the outcome of an attack highly depends on the operational properties of the targeted system at the time of the attack (e.g., generators' settings, amount of renewable resources, and power flows)*. We emphasize this in our simulations by changing the power grid models' parameters to reflect the daily changes in the operational properties of the system.

4.1 Simulations Setup

Our results are based on computer simulations. In particular, we use the MATPOWER [65] and the PowerWorld [7] simulators. MATPOWER is an open-source MATLAB library which is widely used for computing the power flows in power grids. PowerWorld, on the other hand, is an industrial-level software suite that is widely used by the industry for frequency stability analysis of power systems. We used the academic version of Power-

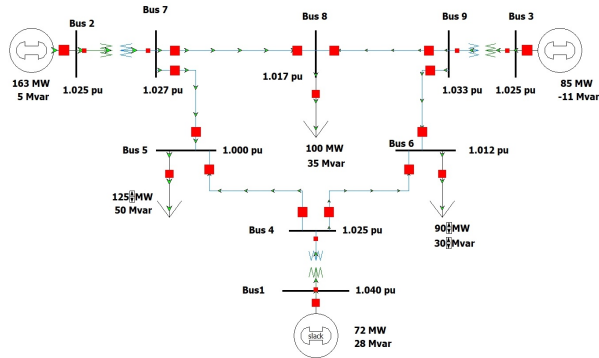


Figure 6: The WSCC 9-bus system. The generators at buses 2 and 3 are the buses with inertia, and the generator at bus 1 is a slack bus with no inertia. The slack bus is a bus in the system that can change its generation to make the power flow equations feasible. The load buses are buses 5, 6, and 8. We consider two operational settings of the WSCC system: (a) high inertia, in which both generators 2 and 3 have inertia constants (H) equal to 15s, and (b) low inertia, in which generators 2 and 3 have inertia constants equal to 5s and 10s, respectively [51, Chapter 3]. In all the simulations, the IEEE type-2 speed-governing model (IEEE-G2) is used for the generators [44].

World.

For frequency stability analysis in PowerWorld, to the best of our knowledge, there are no large-scale real-world power grids available for academic research. Hence, for evaluating the effects of the MadIoT attacks on the system’s frequency, we use the WSCC 9-bus grid model that represents a simple approximation of the Western System Coordinating Council (WSCC)–with 9 buses, 9 lines, and 315MW of demand [35]. Despite its small size, due to the complexity of power systems transient analysis, it is widely used as a benchmark system [22, 48, 52].

For evaluating the effects of MadIoT attacks on the power flows, however, we use the Polish grid which is one of the largest and most detailed publicly available real-world power grids. To the best of our knowledge, there are no other real power grids at this scale and detail available for academic research.⁵We use the Polish grid data at its Summer 2004 peak–with 2736 buses, 3504 lines, and 18GW of demand–and at its Summer 2008 peak–with 3120 buses, 3693 lines, and 21GW of demand. Both are available through the MATPOWER library.

Since the total demand in the WSCC system is 315MW, but the total demand in the Polish grid is about 20GW, for comparison purposes, we focus on the percentage increase/decrease in the demand caused by an attack instead of the number of switching on/off bots. However, if we assume that all the bots are air conditioners, 1MW change in the demand corresponds simply to

⁵Topologies of other power grids may also be available through university libraries, but they are limited to the topology with no extra information on the operational details.

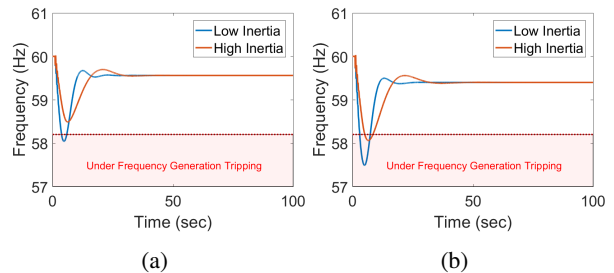


Figure 7: Frequency disturbances due to unexpected demand increases in all the load buses in the WSCC system caused by an adversary, ignoring generators’ frequency cut-off limit (shown by red dashed line). Increase by (a) 23MW and (b) 30MW.

switching on/off 1,000 bots. Therefore, we can define the normalized botnet size in bots/MW to be the number of bots required to perform a successful variation of the MadIoT attack, if the total demand in the system is 1MW. By this definition, it is easy to see that to increase the demand of any system by 1%, an adversary requires 10 bots/MW.

4.2 Frequency Disturbances

In this subsection, we evaluate the first two MadIoT attack variations described in Section 3.2. We consider two operational settings of the WSCC system: (a) high inertia and (b) low inertia (for details see Fig. 6).

4.2.1 200–300 Bots per MW Can Cause Sudden Generation Tripping

In order to show the frequency response of the system to sudden increases in the demand, we simulated the increase of (a) 23MW and (b) 30MW in all the loads for the high inertia and low inertia cases. These values can roughly be considered as 20% and 30% increases in the load buses, respectively. We similarly studied the frequency response of the system to sudden decreases of the demand. Figs. 7 and 8 present the results.

As mentioned in Section 2, the generators are protected from high and low frequency values by protective relays. These values depend on the type of a generator as well as the settings set by the grid operator. Here, we assume the safe frequency interval of 58.2Hz and 61.2Hz which is common in North America (see Fig. 4). Once a generator goes below or above these values, it gets disconnected from the grid by protective relays.

As can be seen in Figs. 7(b) and 8(b), sudden increase or decrease in the load buses by 30% or 20%, respectively, cause the system’s frequency to go below or above the frequency cut-off limits. Hence, an adversary requires 200–300 bots/MW, or in this case 60–90 thousand bots, to perform these attacks.

As can be seen, however, the drop/rise in frequency is higher in the low inertia case (as predicted). Therefore, there are cases in which the frequency may go be-

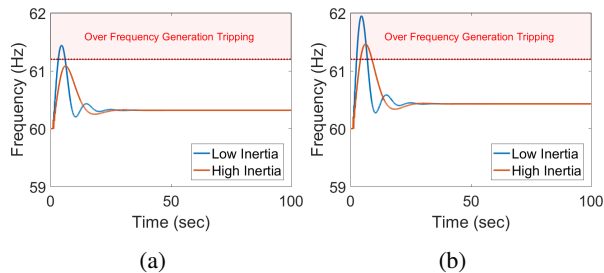


Figure 8: Frequency disturbances due to unexpected demand *decreases* in all the load buses in the WSCC system by an adversary, ignoring generators' frequency cut-off limit (shown by red dashed line). Decrease by (a) 15 MW and (b) 20 MW .

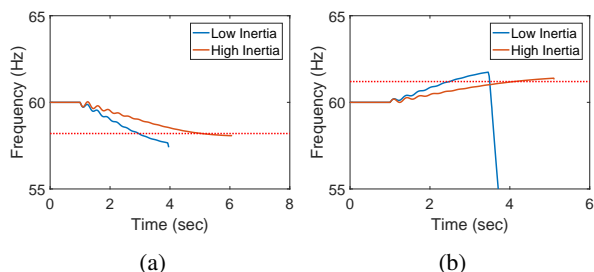


Figure 9: Frequency disturbances due to unexpected demand changes in all the load buses in the WSCC system by an adversary, considering generators' frequency cut-off limits (shown by red dashed lines). (a) Demand increase of 30 MW and (b) demand decrease of 20 MW .

low/above the critical frequency in the low inertia case but may remain in the safe interval in the high inertia case (see Figs. 7(a) and 8(a)). This suggests that *an attack that is not effective today, may be effective tomorrow* if the system's inertia is lower due to a higher rate of renewable generation.

In Figs. 7 and 8, the frequency cut-off limits of the generators are ignored. Hence, the generators are kept online even when the frequency goes beyond the safe operational limits. In reality, however, these generators are disconnected from the grid by the protective relays. Fig. 9 presents the frequency response of the system when the protective relays are enabled for the cases shown in Figs. 7(b) and 8(b). As can be seen, the grid completely shuts down and the simulations stop in less than 10 seconds due to disconnection of the generators.

Simulation results in this subsection demonstrate that the effectiveness of an attack in causing a critical frequency disturbance depends on the attack's scale as well as the system's total inertia at the time of the attack.

4.2.2 100–200 Bots per MW Can Disrupt the Grid Re-start

Once there is a blackout, the grid operator needs to restart the system as soon as possible (a.k.a. a black start). As mentioned in Section 3.2, due to frequency instability of the system at the black start, the restarting process is

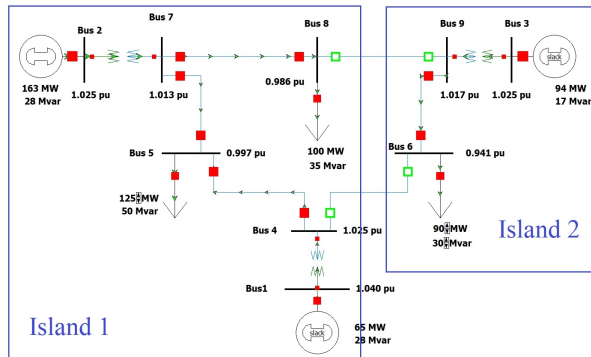


Figure 10: The WSCC 9-bus system during the black start.

usually done by restarting the grid in parallel in disconnected islands and then reconnecting the islands.

Fig. 10 shows one way of partitioning the WSCC system into two islands. We assume that initially the grid operator could restart the two islands and stabilize the frequency at 60 Hz . Then, before the two islands are reconnected, an adversary increases the demand at all the load buses with the same amount (see Fig. 11).

The attack is performed at time 30 and the two islands are reconnected at time 50. As can be seen in Fig. 11(a), when there are no attacks, the two islands are reconnected with an initial small disturbance in the frequency and then the system reaches a stable state.

Fig. 11(b) shows the frequency of the system after 20 MW increase in all the load buses at time 30. In this case, the frequency goes slightly below the minimum safe limit, but it is common in the black start process that the generators' lower (upper) frequency limits are set to lower (higher) levels than usual. Hence, the system may reach a stable state in this case as well.

As can be seen in Fig. 11(c), a 30 MW increase in all the loads causes a large disturbance in the frequency, but as the two islands are reconnected the system's frequency is completely destabilized. These substantial deviations from safe frequency ranges can cause serious damage to the generators and are not permitted even in the black start process. Hence, in this case the system returns to the blackout stage. Even if the grid operator decides not to reconnect the two islands due to the frequency disturbances, Fig. 11(d) shows a significant drop in the second island's frequency that results in disconnection of the generators. Therefore, even if the big drop in frequency of island 1 (1 Hz below the safe limit) is acceptable during the black start, island 2 goes back to the blackout state.

For comparison purposes and to reflect on the role of the operational properties of the system on the outcome of an attack, we repeated the same set of simulations with different maximum power outputs for the generators' governors (see Fig. B.1 in the appendix). We observed that under the new settings, demand increases of

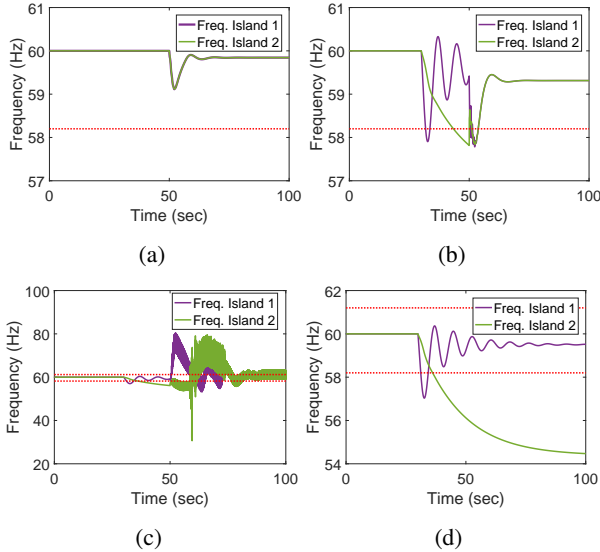


Figure 11: Frequency disturbances during the black start due to unexpected increases in all the load buses by an adversary, ignoring generators’ frequency cut-off limits (shown by red dashed lines). (a) Normal black start in the absence of an adversary. (b) Demand increases of $20MW$ at the load buses before the reconnection of the two islands. (c) Demand increases of $30MW$ at the load buses before the reconnection of the two islands. (d) Demand increases of $30MW$ at the load buses without attempting to reconnect the two islands due to frequency instabilities.

up to $10MW$ results is a successful black start, unlike the previous case which could handle demand increases of $20MW$ at all the loads. Hence, an adversary requires at least 100–200 bots/ MW , or in this case 30–60 thousand bots, to increase the demand at all the loads by 10–20% and disrupt the black start. Here again *we observe that the operational properties of the grid play an important role in the outcome of an attack.*

4.3 Line Failures and Cascades

In this subsection, we demonstrate the effectiveness of the third and the fourth variations of the MadIoT attacks described in Section 3.2. For simulating the cascading line failures, we use the MATLAB code developed by Cetinay et al. [18]. We had to slightly change the code to make it functional in the scenarios studied in this paper. To evaluate the severity of the cascade, we define *outage* as the percent of the demand affected by the power outage at the end of the cascade over the initial demand.

4.3.1 Only 10 Bots per MW Can Initiate a Cascading Failure Resulting in 86% Outage

As described in Section 3.2, once an adversary causes a sudden increase in the demand, if it does not result in a major frequency drop, the primary controllers at generators are automatically activated to compensate for the imbalance in the supply and demand. Despite balancing

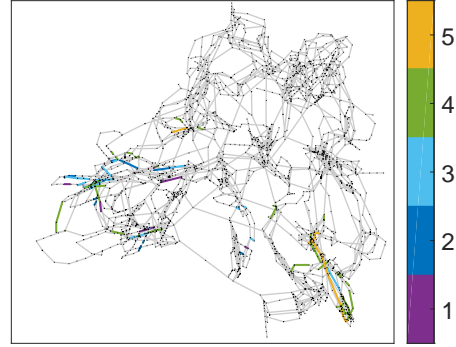


Figure 12: The cascading line failures initiated by a 1% increase in the demand in the Polish grid 2008 by an adversary (colors show the cascade step at which a line fails). It caused failures in 263 lines and 86% outage.

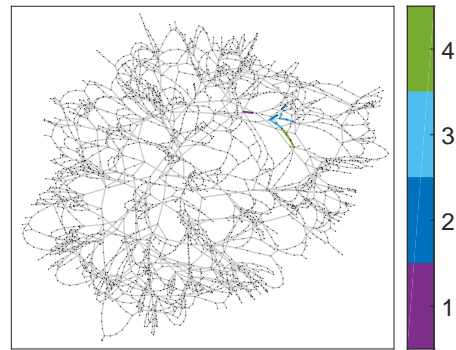


Figure 13: The cascading line failures initiated by a 10% increase in the demand in the Polish grid 2004 by an adversary (colors show the cascade step at which a line fails). It caused failures in 11 lines and 46% outage.

the supply and demand, since this balancing is unplanned, it may cause line overloads.

To demonstrate this, we assume that an adversary increases the demand at all the load buses by 1%. We also assume that all the generators contribute proportionally to their capacities to compensate for this sudden increase in the demand. This attack results in a single line failure in the Polish grid 2004 but no outages. However, as can be seen in Fig. 12, the same attack on the Polish grid 2008 results in the cascade of line failures that lasts for 5 rounds, causes 263 line failures, and 86% outage. The 1% increase in the total demand in the Polish grid 2008 is roughly equal to $210MW$, requiring the adversary to access to 10 bots/ MW which is about 210 thousand air conditioners in this case. This number is equal to 1.5% of the total number of households in Poland [58].

Since the Polish grid 2004 showed a good level of robustness against the 1% increase attack, we re-evaluated its robustness against a 10% increase in the demand. Fig. 13 shows the resulting line failures and the subsequent cascade caused by this attack. It can be seen that this attack causes much more damage with 11 line fail-

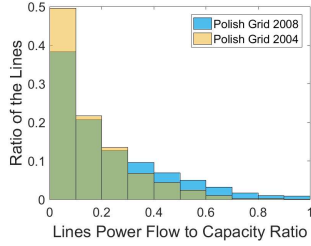


Figure 14: Histogram of the Polish grid lines' power flow to capacity ratio in Summer 2004 compared to Summer 2008.

ures and 46% outage. Despite the effectiveness of the second attack, the Polish grid 2004 shows greater level of robustness than the Polish grid 2008 even under a 10-time stronger attack. Although this may be due to many factors such as online generator locations and their values, topology of the grid, and even number of lines [54], one possible factor is *how initially saturated the power lines are*.

Fig. 14 presents the histogram of the Polish grid lines' power flow to capacity ratio in Summer 2004 compared to Summer 2008. There are about 10% more lines with flow to capacity ratio below 0.1 in the Polish grid 2004 compared to the Polish grid 2008. Consequently, there are more lines with power flow to capacity ratio greater than 0.3 in the Polish grid 2008 than in the Polish grid 2004 (to see the locations of the near saturated lines see Fig. B.2 in the appendix). This clearly demonstrates that a small increase in the demand is more likely to cause line overloads in the Polish grid 2008 than in the Polish grid 2004 (as observed in Figs.12 and 13).

Overall, as in the previous subsection, the results demonstrate that the effectiveness of an attack depends on the status of the grid at the time of the attack. However, *unlike the large botnet size (about 300 bots/MW) required to cause a blackout from frequency instability in the system, we observe here that even botnet size of 10 bots/MW can result in a significant blackout depending on the grid's operational properties*. Albeit the blackouts caused by frequency instabilities happen much faster (within seconds) than those caused by cascading line failures (within minutes or even hours).

4.3.2 Only 4 Bots per MW Can Initiate a Cascading Failure Resulting in 85% Outage by Redistributing the Demand

Another way of causing line failures and possibly cascading line failures in the grid is by redistributing the demand without increasing the total demand. As mentioned in Section 3.2, the advantage of this attack is that it may have a similar effect to the demand increase attack without attracting the grid operators' attention due to frequency disturbances.

Here, an adversary focuses only on the loads with de-

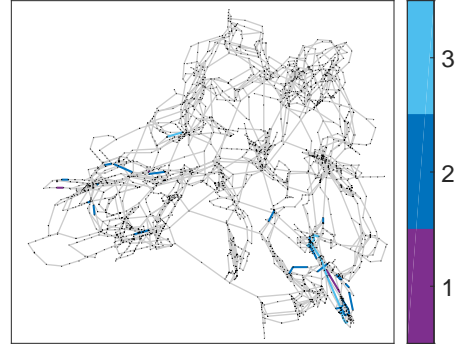


Figure 15: The cascading line failures initiated in the Polish grid 2008 by redistributing the demand by an adversary. Demand of the loads buses with demand greater than $20MW$ are changed by with a Gaussian distribution with zero mean and standard deviation $1MW$ (colors show the cascade step in which a line fails). It caused failures in 77 lines and 85% outage.

mand greater than $20MW$. This can be estimated by the adversary from the total number of IoT bots in a city or a town. The number of bots is correlated with the population of an area and therefore the total demand. Hence, an adversary detects these load buses and decreases or increases the demands by a random value such that the total demand increase and decrease sum up approximately to zero. We assume this can be done by randomly increasing or decreasing the demand by a Gaussian random variable with zero mean and selected standard deviation.

Again, the Polish grid 2004 showed a great level of robustness against these attacks. Even if an adversary decreases or increases the demand randomly by a Gaussian random variable with zero mean and standard deviation $10MW$ at loads with demand greater than $20MW$, it only results in three line failures without any outages. However, the same attack with 10-time smaller changes, results in serious damage to the Polish grid 2008. As can be seen in Fig. 15, making only small changes with standard deviation of $1MW$ at load buses with demands greater $20MW$ results in cascading line failures with 77 line failures and outage of 85%. The total absolute value of the demand changes in this attack was about $80MW$ which means that *an adversary only requires 4 bots/MW, or in this case 80 thousand bots, to perform such an attack*.

Although these changes are made randomly, due to the stealthy nature of these attacks they can be repeated without attracting any attention until they are effective.

4.3.3 Only 15 Bots per MW Can Fail a Tie-line by Increasing (Decreasing) the Demand of the Importing (Exporting) ISOs

In order to demonstrate an attack on the tie-lines as described in Section 3.2, since we do not have access to the European grid or the U.S. Eastern Interconnection, we modified the Polish grid 2008 in a principled manner to

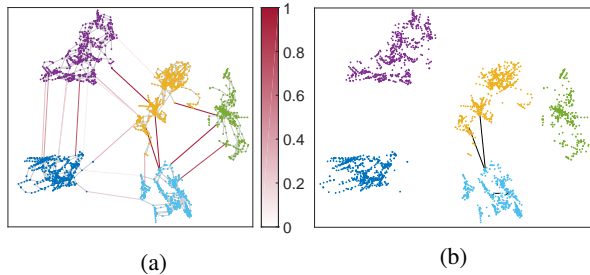


Figure 16: Tie-line vulnerabilities in the partitioned Polish grid 2008. (a) The ratios of tie-lines’ power flows to their nominal capacity. (b) Failures in the tie-lines between the yellow area and the light blue area caused by decreasing the demand by 1.5% in the former and increasing the demand by 1.5% in the latter by an adversary. Failed lines are shown in black.

represent a few neighboring ISOs in Europe connected by a few tie-lines.

First, we used a spectral clustering method to partition the Polish grid into 5 areas with a few connecting tie-lines. This is done using MATLAB’s Community Detection Toolbox [34, 36]. Since the Polish grid does not inherently have 5 areas, however, the number of tie-lines between areas is slightly more than those of the European grid or Eastern Interconnection. Therefore, we removed one fifth of the tie-lines. In order to make the power flows feasible then, we reduced the total supply and demand by 60% and increased the capacity on the lines that were overloaded.

Fig. 16(a) shows the modified grid along with the ratios of tie-lines’ power flows to their nominal capacities. As can be seen, similarly to the real grid operation, some of these tie-lines are carrying power flows near their capacities. These lines—which can be detected through some of the ISOs’ websites [5]—are the most vulnerable to this variation of the MadIoT attacks.

For example, as can be seen in Fig. 16(a), the two lines that are connecting the yellow area to the light blue area are carrying power flows near their capacities. Therefore, increasing the demand in the light blue area and decreasing the demand in the yellow area (corresponding to the direction of the power flow on the lines) can potentially result in those lines tripping. It can be seen in Fig. 16(b) that a 1.5% decrease in the demand of the yellow area and a 1.5% increase of the demand in the light blue area by an adversary results in the failure of the two tie-lines (additional attacks on the other tie-lines are demonstrated in Figs. B.3(a) and B.3(b) in the appendix). Hence, an adversary can cause a failure in a tie-line by only a botnet of size 15 bots/ MW , or in this case 60 thousand bots (30 thousand bots at each end of the tie-line).

Since the tie-lines usually carry substantial amounts of power, failure in these lines can result in cascade of line failures in other lines and eventually in disconnection of an ISO from the interconnection. Such a disconnection

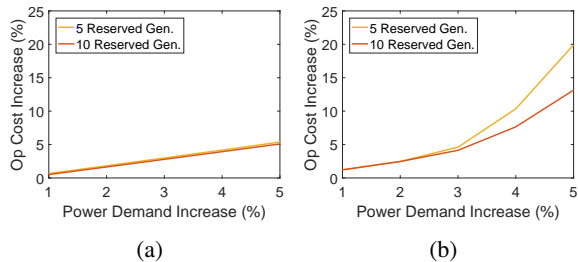


Figure 17: Increase in the operating cost of the Polish grid 2004 by an adversary. The initial demand is 10% higher than the original demand during the Summer 2004 morning peak. (a) If the operating costs of the reserve generators are linear functions $c_1(x) = 100x$, and (b) if the operating costs of the reserve generators are quadratic functions $c_2(x) = 5x^2 + 100x$.

may result in a huge imbalance in the supply and demand values and in uncontrollable frequency drop leading to an inevitable blackout.

Attacks on the tie-lines are an effective approach when an adversary has a limited number of bots. By disconnecting an ISO from its neighboring ISOs, an adversary can cause a huge demand deficit in the targeted ISO and possibly a large-scale blackout.

4.4 Increasing the Operating Cost

In this final subsection, we evaluate the last variation of the MadIoT attacks described in Section 3.2. In this variation of the attacks, an adversary increases the demand and not to necessarily cause a blackout, but rather to significantly increase the operating cost of the grid in favor of a utility in the electricity market.

4.4.1 50 Bots per MW Can Increase the Operating Cost by 20%

For these simulations, we use the Polish grid in Summer 2004. However, in order to mainly focus on the cost related issues, we increase the line capacities to make sure that the attack causes no line overloads. To simulate the system in its peak demand state, we increase the initial demand by 10% to make the demand before the attack close to the online generators’ generation capacity.

We assume that the sudden increase in the demand caused by the attack can temporarily be handled by the primary controller and no large frequency drops as in Section 4.2 happen in any of the scenarios here. Therefore, our focus is on the cost of the required reserve generators for providing the additional power and returning the system’s frequency back to 60 Hz (or 50 Hz).

We consider two cases, one with 5 reserve generators, and the other one with 10. We also consider two possible cost functions for the reserve generators: $c_1(x) = 100x$ and $c_2(x) = 5x^2 + 100x$, in which x is in MW and the $c_i(x)$ s are in $\$/hr$. The linear and quadratic cost functions are the most common functions for approximating the generation costs [62, Chapter 3]. The $c_1(x)$ is selected

similarly to cost function of the high-cost online generators in the grid before the attack and the $c_2(x)$ is selected to capture the start-up cost of the reserve generators as well as their higher cost compared to the online generators.

Fig. 17 shows the increase in the total cost given the two cost functions. As can be seen, in the worst-case scenario, a 5% increase in the demand—which requires 50 bots/ MW , or in this case 1 million bots—can result in about a 20% increase in the operating cost of the grid (see the yellow line in Fig. 17(b)). This is four times higher than the best-case scenario (see the orange line in Fig. 17(a)) which is similar to the normal increase in the operating cost when no reserve generators are needed.

We observe that the effectiveness of the attack in increasing the cost depends on the total number of reserve generators as well as their generation cost functions.

5 Countermeasure Sketches

Although we are not aware of any rigorous countermeasures against the MadIoT attacks, in this section, we briefly provide a set of suggestions both in the power grid operation side and in the IoT design side to reduce the effectiveness of these attacks.

5.1 Power Grid Side

One of the most important properties of the MadIoT attacks, as mentioned in Section 3.3, is that grid operators, in general, are not prepared for these types of attacks. Hence, these types of attacks are not part of the contingency list of the power grid operators. Our first suggestion is for the grid operators to consider the MadIoT attacks in their contingency list and prepare for them. Such preparations can be directly incorporated into their already existing day-ahead planning tools to ensure that their systems have for example enough *inertia* (or *spinning reserve*) and the power lines have enough extra capacity to minimize the effects of a potential attacks. Although this might initially increase the grid operating cost, by developing more efficient planning tools and applying recent advances in designing *virtual inertia* for power systems [32], these costs can be reduced in the future. Thus, our suggestion for system operators is to push for more research in that direction in order to make their systems more robust to potential MadIoT attacks.

To minimize costs, the grid operators should also *have an accurate estimate of the total number of high wattage IoT devices in their system and accordingly the scale of a potential attack*, without being overprotective.

Since this is a new type of attack, enabled by the ubiquity of IoT devices, our last suggestion for the systems operators is *to revisit their online data and to find secure ways to release their data without revealing any critical information* that can be used by an adversary to improve

the effectiveness of an attack.

5.2 IoT Side

The security challenges facing IoT devices are much more difficult to deal with. There are many ways an adversary can access a smart appliance. An adversary can directly get access to the device, or get access to the mobile phone, tablet, or a thermostat that controls that device, or with the ubiquity of digital home assistant devices such as Amazon Alexa or Google Home, an adversary can control smart appliances by getting access to these devices. Any of these devices can be a breaching point for an adversary. Hence, *coherent security measures are needed to protect almost all the devices within a home network against an adversary.*

Thus, in the IoT side, more research is required to study the vulnerability of IoT devices and networks, and to protect them against cyber attacks.

6 Related Work

The security and vulnerability of the IoT against cyber attacks has been widely studied [21, 42, 45, 50, 53, 57, 63]. In a recent study of the DDoS attack by the Mirai botnet [12], Antonakakis et al. showed that due to poor security measures in the IoT devices, such as easy to guess default passwords, an attacker could get access to about 600 thousand devices from cameras to DVRs and routers in a very short period. Similar studies had previously shown that Honeywell home controllers (including thermostats) could easily be compromised due to a pair of bugs in their authentication system [6]. It was also shown by Hernandez et al. that the lack of proper hardware protections in Nest thermostats allows attackers to install malicious software on these devices [33]. The vulnerability of Arduino Yun microcontrollers—used in some IoT devices—to cyber attacks was also revealed by Pastrana et al. [47].

In an interesting recent work [64], Zhang et al. demonstrated that home assistant devices can be controlled by an adversary using inaudible voice commands. In another recent work [49], Ronen et al. demonstrated that the smart lights within a city can potentially be compromised by creating a worm that can affect all the lamps using Zigbee. The security of mobile applications that control IoT devices has also been studied [28, 43]. In a comprehensive work [28], Fernandes et al. studied security of all Samsung-owned SmartThings apps and demonstrated that due to the security flaws in these applications, they could perform attacks like disabling vacation mode of a smart home. Naveed et al. also demonstrated that malicious apps on Android devices can freely *mis-bond* with any external IoT devices and control them [43].

Power systems' vulnerability to failures and attacks has been widely studied in the past few years [14, 17, 18, 23, 54]. In a recent work [29], Garcia et al. introduced Har-

vey, malware that affects power grid control systems and can execute malicious commands. Theoretical methods for detecting cyber attacks on power grids and recovering information after such attacks have also been developed [15, 20, 37, 39, 40, 55]. However, most of the previous work has focused on the attacks that directly target the power grid’s physical infrastructure or its control system.

The interdependency between failures in power grids and communication networks, and their propagation has also been recently studied [16, 38, 46], but these works focused on attacks and failures that target both the power grid’s and the communication network’s physical infrastructure at the same time.

Load altering attacks on smart meters and large cloud servers has been first introduced by Mohsenian et al. [41]. Their work was mostly focused on the cost of protecting the grid against such attacks at loads. In contrast, we have analyzed the consequence of such attacks and introduced practical ways that they can be performed. Amini et al. [11] have also recently studied the effects of load altering attacks on the dynamics of the system and ways to use the system’s frequency as feed-back to improve an attack. In two very recent papers, Dvorkin and Sang [24], and Dabrowski et al. [19] independently revealed the possibility of exploiting compromised IoT devices to disrupt normal operation of the power grid. Dvorkin and Sang [24] modeled their attack as an optimization problem for the attacker—with complete knowledge of the grid—to cause circuit breakers to trip in the distribution network. In contrast, we have focused on black-box attacks on transmission networks. Dabrowski et al. [19] studied the effect of demand increases caused by remotely activating CPUs, GPUs, hard disks, screen brightness, and printers on the frequency of the European power grid. *To the best of our knowledge, however, the work presented in this paper provides the most coherent and complete study on the effects of potential attacks on the power grid using high wattage IoT devices.*

There is another line of research that focuses on privacy of the customers in the presence of smart power meters which is beyond the scope of our paper [30].

7 Limitations and Future Work

In this work, we have analyzed the potential consequences of the MadIoT attacks on the operation of the power grid. However, our study has some limitations, and by addressing them one can provide a clearer picture of the threats facing the grid now and in the future. First, as mentioned in Section 4, we have only used publicly available data sets that may not exactly reflect the characteristics of all existing power grids. Therefore, the number of bots listed in Table 2 may not be enough to cause significant damage to all power grids. More detailed analysis of MadIoT attacks should be performed by system operators

with access to the details of their systems.

Second, in our studies, we have not fully considered the existing control mechanisms for minimizing the subsequent effects of an initial failure (e.g., preventive load-shedding mechanisms). Hence, our cascading failures analysis may only reflect the worst case scenario.

Third, some of these high wattage IoT devices like air conditioners, have very large capacitors. Hence, it takes these devices 10 to 15 seconds to reach their maximum capacities. Therefore, it might be challenging to cause an abrupt increase in the demand and subsequently sudden drop in the frequency using these devices. Nevertheless, other smart devices like water heaters that are *resistive* loads can still be used for such purposes. Moreover, other varieties of the MadIoT attacks that do not require *synchronicity* on the scale of seconds (e.g., line failures) can still be performed using air conditioners.

Finally, unlike DDoS attacks, for the MadIoT attacks, the IoT bots should all be geographically located within boundaries of a power system. Hence, although the numbers of bots in Table 2 are achievable considering recent botnet sizes (e.g., the Mirai botnet), it might be much more challenging to reach these numbers within a targeted geographical location.

8 Conclusions

We have studied the collective effects of vulnerable high wattage IoT devices and have shown that once compromised, an adversary can utilize these devices to perform attacks on the power grid. We have revealed a new class of attacks on the power grid using an IoT botnet called Manipulation of demand via IoT (MadIoT) attacks. We have demonstrated via state-of-the-art simulators that these attacks can result in local outages as well as large-scale blackouts in the power grid depending on the scale of the attack as well as the operational properties of the grid. Moreover, we have shown that the MadIoT attacks can also be used to increase the operating cost of the grid to benefit a few utilities in the electricity market.

We hope that our work raises awareness of the significance of these attacks to grid operators, smart appliance manufacturers, and systems security experts in order to make the power grid (and other interdependent networks) more secure against cyber attacks. This is especially critical in the near future when more *smart* appliances with the ability to connect to the Internet are going to be manufactured. In particular, our work leads to following recommendations for the research community:

Power systems’ operation: Power systems’ operators should rigorously analyze the effects of potential MadIoT attacks on their systems and develop preventive methods to protect their systems. Initiating a data sharing platform between academia and industry may expedite these developments in the future.

IoT security: As shown by both presented MadIoT attacks and the Mirai botnet, insecure IoT devices can have devastating consequences that go far beyond individual security/privacy losses. This necessitates a rigorous pursuit of the security of IoT devices, including regulatory frameworks.

Interdependency: Our work demonstrates that interdependency between infrastructure networks may lead to hidden vulnerabilities. System designers and security analysts should explicitly study threats introduced by interdependent infrastructure networks such as water, gas, transportation, communication, power grid, and several other networks.

Acknowledgments

This work was supported in part by the U.S. National Science Foundation under Grants DMS-1736417, ECCS-1549881, and CNS-1553437, and Office of Naval Research YIP Award. We also thank anonymous reviewers for their helpful comments.

References

- [1] Amazon Echo. <https://www.amazon.com/all-new-amazon-echo-speaker-with-wifi-alex-dark-charcoal/dp/B06XCM9LJ4>. Accessed: Jan. 2018.
- [2] Aquanta: Heat water when you need it, save money when you don't. <https://aquanta.io/>. Accessed: Jan. 2018.
- [3] GE Wi-Fi connect appliances. <http://www.geappliances.com/ge/connected-appliances/>. Accessed: Jan. 2018.
- [4] Google Home. https://store.google.com/product/google_home. Accessed: Jan. 2018.
- [5] New York Independent System Operator (NYISO). <http://www.nyiso.com/public/index.jsp>. Accessed: Jan. 2018.
- [6] Pair of bugs open Honeywell home controllers up to easy hacks. <https://threatpost.com/pair-of-bugs-open-honeywell-home-controllers-up-to-easy-hacks/113965/>. Accessed: Jan. 2018.
- [7] PowerWorld Simulator. <https://www.powerworld.com/>. Accessed: Jan. 2018.
- [8] Tado intelligent AC control. <https://www.tado.com/us/>. Accessed: Jan. 2018.
- [9] The Federal Energy Regulatory Commission (FERC) and the North American Electric Reliability Corporation (NERC). Arizona-Southern California Outages on September 8, 2011. <http://www.ferc.gov/legal/staff-reports/04-27-2012-ferc-nerc-report.pdf>. Accessed: Jan. 2018.
- [10] U.S. Energy Information Administration (EIA). <https://www.eia.gov/>. Accessed: Jan. 2018.
- [11] AMINI, S., PASQUALETTI, F., AND MOHSENIAN-RAD, H. Dynamic load altering attacks against power system stability: Attack models and protection schemes. *IEEE Trans. Smart Grid* 9, 4 (2018), 2862–2872.
- [12] ANTONAKAKIS, M., APRIL, T., BAILEY, M., BERNHARD, M., BURSZEIN, E., COCHRAN, J., DURUMERIC, Z., HALDERMAN, J. A., INVERNIZZI, L., KALLITSIS, M., ET AL. Understanding the Mirai botnet. In *Proc. USENIX Security Symposium'17* (Aug. 2017).
- [13] AUSTRALIAN ENERGY MARKET OPERATOR (AEMO). Black system South Australia 28 september 2016. https://www.aemo.com.au/-/media/Files/Electricity/NEM/Market_Notices_and_Events/Power_System_Incident_Reports/2017/Integrated-Final-Report-SA-Black-System-28-September-2016.pdf. Accessed: Jan. 2018.
- [14] BIENSTOCK, D. *Electrical Transmission System Cascades and Vulnerability: An Operations Research Viewpoint*. SIAM, 2016.
- [15] BIENSTOCK, D., AND ESCOBAR, M. Computing undetectable attacks on power grids. *ACM PER* 45, 2 (2017), 115–118.
- [16] BULDYREV, S., PARSHANI, R., PAUL, G., STANLEY, H., AND HAVLIN, S. Catastrophic cascade of failures in interdependent networks. *Nature* 464, 7291 (2010), 1025–1028.
- [17] CARRERAS, B., LYNCH, V., DOBSON, I., AND NEWMAN, D. Critical points and transitions in an electric power transmission model for cascading failure blackouts. *Chaos* 12, 4 (2002), 985–994.
- [18] CETINAY, H., SOLTAN, S., KUIPERS, F. A., ZUSSMAN, G., AND VAN MIEGHEM, P. Analyzing cascading failures in power grids under the AC and DC power flow models. In *Proc. IFIP Performance'17* (Nov. 2017).
- [19] DABROWSKI, A., ULLRICH, J., AND WEIPPL, E. R. Grid shock: Coordinated load-changing attacks on power grids: The non-smart power grid is vulnerable to cyber attacks as well. In *Proc. ACM ACSAC'17* (Dec. 2017).
- [20] DÁN, G., AND SANDBERG, H. Stealth attacks and protection schemes for state estimators in power systems. In *Proc. IEEE SmartGridComm'10* (2010).
- [21] DENNING, T., KOHNO, T., AND LEVY, H. M. Computer security and the modern home. *Commun. ACM* 56, 1 (2013), 94–103.
- [22] DOBAKSHARI, A. S., AND RANJBAR, A. M. A novel method for fault location of transmission lines by wide-area voltage measurements considering measurement errors. *IEEE Trans. Smart Grid* 6, 2 (2015), 874–884.
- [23] DOBSON, I. Cascading network failure in power grid blackouts. *Encyclopedia of Systems and Control* (2015), 105–108.
- [24] DVORKIN, Y., AND GARG, S. IoT-enabled distributed cyber-attacks on transmission and distribution grids. In *Proc. NAPS'17* (Sept 2017).
- [25] EUROPEAN NETWORK OF TRANSMISSION SYSTEM OPERATORS FOR ELECTRICITY (ENTSOE). Frequency stability evaluation criteria for the synchronous zone of continental Europe. https://www.entsoe.eu/Documents/SOC%20documents/RGCE_SPD_frequency_stability_criteria_v10.pdf. Accessed: Jan. 2018.
- [26] EUROPEAN NETWORK OF TRANSMISSION SYSTEM OPERATORS FOR ELECTRICITY (ENTSOE). Continental Europe operation handbook, 2004. <https://www.entsoe.eu/publications/system-operations-reports/operation-handbook/Pages/default.aspx>. Accessed: Jan. 2018.
- [27] FEDERAL ENERGY REGULATORY COMMISSION AND OTHERS. *Energy Primer, a Handbook of Energy Market Basics*. 2012.
- [28] FERNANDES, E., JUNG, J., AND PRAKASH, A. Security analysis of emerging smart home applications. In *Proc. IEEE S&P'16* (2016), pp. 636–654.
- [29] GARCIA, L., BRASSER, F., CINTUGLU, M. H., SADEGHI, A.-R., MOHAMMED, O., AND ZONOZ, S. A. Hey, my malware knows physics! attacking PLCs with physical model aware rootkit. In *Proc. NDSS'17* (2017).

- [30] GIACONI, G., GÜNDÜZ, D., AND POOR, H. V. Privacy-aware smart metering: Progress and challenges. *IEEE Signal Process. Mag. (to appear)* (2018).
- [31] GLOVER, J. D., SARMA, M. S., AND OVERBYE, T. *Power System Analysis & Design, SI Version*. Cengage Learning, 2012.
- [32] GROSS, D., BOLOGNANI, S., POOLLA, B. K., AND DÖRFLER, F. Increasing the resilience of low-inertia power systems by virtual inertia and damping. In *Proc. IEEE IREP'17* (2017).
- [33] HERNANDEZ, G., ARIAS, O., BUENTELLO, D., AND JIN, Y. Smart nest thermostat: A smart spy in your home. *Black Hat USA* (2014).
- [34] HESPANHA, J. P. An efficient Matlab algorithm for graph partitioning. *Technical Report* (2004). <https://www.ece.ucsb.edu/~hespanha/published/tr-ell-gp.pdf>. Accessed: Jan. 2018.
- [35] ILLINOIS CENTER FOR A SMARTER ELECTRIC GRID (ICSEG). Power test cases. <http://icseg.iti.illinois.edu/power-cases/>. Accessed: Jan. 2018.
- [36] KEHAGIAS, A. Community detection toolbox. <https://www.mathworks.com/matlabcentral/fileexchange/45867-community-detection-toolbox>. Accessed: Jan. 2018.
- [37] KIM, J., TONG, L., AND THOMAS, R. J. Subspace methods for data attack on state estimation: A data driven approach. *IEEE Trans. Signal Process.* 63, 5 (2015), 1102–1114.
- [38] KORKALI, M., VENEMAN, J. G., TIVNAN, B. F., BAGROW, J. P., AND HINES, P. D. Reducing cascading failure risk by increasing infrastructure network interdependence. *Sci. Rep.* 7 (2017).
- [39] LI, S., YILMAZ, Y., AND WANG, X. Quickest detection of false data injection attack in wide-area smart grids. *IEEE Trans. Smart Grid* 6, 6 (2015), 2725–2735.
- [40] LIU, Y., NING, P., AND REITER, M. K. False data injection attacks against state estimation in electric power grids. *ACM Trans. Inf. Syst. Secur.* 14, 1 (2011), 13.
- [41] MOHSENIAN-RAD, A.-H., AND LEON-GARCIA, A. Distributed internet-based load altering attacks against smart power grids. *IEEE Trans. Smart Grid* 2, 4 (2011), 667–674.
- [42] NAEINI, P. E., BHAGAVATULA, S., HABIB, H., DEGELING, M., BAUER, L., CRANOR, L., AND SADEH, N. Privacy expectations and preferences in an IoT world. In *Proc. SOUPS'17* (2017).
- [43] NAVEED, M., ZHOU, X.-Y., DEMETRIOU, S., WANG, X., AND GUNTER, C. A. Inside job: Understanding and mitigating the threat of external device mis-binding on android. In *Proc. NDSS'14* (2014).
- [44] NEPLAN-POWER SYSTEMS ANALYSIS. Turbine-governor models. http://www.neplan.ch/wp-content/uploads/2015/08/Nep_TURBINES_GOV.pdf. Accessed: Jan. 2018.
- [45] NIA, A. M., AND JHA, N. K. A comprehensive study of security of internet-of-things. *IEEE Trans. Emerg. Topics Comput.* 5, 4 (2017), 586–602.
- [46] PARANDEHGHEIBI, M., AND MODIANO, E. Robustness of interdependent networks: The case of communication networks and the power grid. In *Proc. IEEE GLOBECOM'13* (2013).
- [47] PASTRANA, S., RODRIGUEZ-CANSECO, J., AND CALLEJA, A. ArduWorm: A functional malware targeting Arduino devices. *COSEC Computer Security Lab* (2016).
- [48] RAMIREZ, L., AND DOBSON, I. Monitoring voltage collapse margin with synchrophasors across transmission corridors with multiple lines and multiple contingencies. In *Proc. IEEE PES-GM'15* (2015).
- [49] RONEN, E., SHAMIR, A., WEINGARTEN, A.-O., AND O'FLYNN, C. IoT goes nuclear: Creating a ZigBee chain reaction. In *Proc. IEEE S&P'17* (2017).
- [50] SACHIDANANDA, V., TOH, J., SIBONI, S., SHABTAI, A., AND ELOVICI, Y. Poster: Towards exposing internet of things: A roadmap. In *Proc. ACM CCS'16* (2016).
- [51] SAUER, P., AND PAI, M. *Power System Dynamics and Stability*. Prentice Hall, 1998.
- [52] SHARMA, A., SRIVASTAVA, S., AND CHAKRABARTI, S. Testing and validation of power system dynamic state estimators using real time digital simulator (RTDS). *IEEE Trans. Power Syst.* 31, 3 (2016), 2338–2347.
- [53] SIMPSON, A. K., ROESNER, F., AND KOHNO, T. Securing vulnerable home IoT devices with an in-hub security manager. In *Proc. IEEE PerCom'17* (2017).
- [54] SOLTAN, S., MAZAUIC, D., AND ZUSSMAN, G. Analysis of failures in power grids. *IEEE Trans. Control Netw. Syst.* 4, 3 (2017), 288–300.
- [55] SOLTAN, S., YANNAKAKIS, M., AND ZUSSMAN, G. Joint cyber and physical attacks on power grids: Graph theoretical approaches for information recovery. In *Proc. ACM SIGMETRICS'15* (June 2015).
- [56] STATISTA. Number of homes with smart thermostats in North America from 2014 to 2020 (in millions). <https://www.statista.com/statistics/625868/homes-with-smart-thermostats-in-north-america/>. Accessed: Jan. 2018.
- [57] SURBATOVICH, M., ALJUR Aidan, J., BAUER, L., DAS, A., AND JIA, L. Some recipes can do more than spoil your appetite: Analyzing the security and privacy risks of ifttt recipes. In *Proc. WWW'17* (2017).
- [58] THE UNITED NATIONS. Demographic yearbook, 2017. <https://unstats.un.org/unsd/demographic-social/products/dyb/dybcensusdata.cshtml>. Accessed: Jan. 2018.
- [59] UNION FOR THE COORDINATION OF THE TRANSMISSION OF ELECTRICITY (UCTE). Final report of the investigation committee on the 28 September 2003 blackout in Italy. http://www.rae.gr/old/cases/C13/italy/UCTE_rept.pdf. Accessed: Jan. 2018.
- [60] U.S.-CANADA POWER SYSTEM OUTAGE TASK FORCE. Report on the August 14, 2003 blackout in the United States and Canada: Causes and recommendations. <https://energy.gov/sites/prod/files/oeprod/DocumentsandMedia/BlackoutFinal-Web.pdf>. Accessed: Jan. 2018.
- [61] WANG, N., ZHANG, J., AND XIA, X. Energy consumption of air conditioners at different temperature set points. *Energy and Buildings* 65 (2013), 412–418.
- [62] WOOD, A. J., AND WOLLENBERG, B. F. *Power Generation, Operation, and Control*. John Wiley & Sons, 2012.
- [63] YU, T., SEKAR, V., SESHAN, S., AGARWAL, Y., AND XU, C. Handling a trillion (unfixable) flaws on a billion devices: Rethinking network security for the internet-of-things. In *Proc. ACM Hot-Nets'15* (2015).
- [64] ZHANG, G., YAN, C., JI, X., ZHANG, T., ZHANG, T., AND XU, W. DolphinAttack: Inaudible voice commands. In *Proc. ACM CCS'17* (2017).
- [65] ZIMMERMAN, R. D., MURILLO-SÁNCHEZ, C. E., AND THOMAS, R. J. MATPOWER: Steady-state operations, planning, and analysis tools for power systems research and education. *IEEE Trans. Power Syst.* 26, 1 (2011), 12–19.

Appendix

A Historical Blackouts Details

In this appendix, we briefly review a few of the recent blackouts in the power grids around the world to further demonstrate the potential effectiveness of the MadIoT attacks.

A.1 The 2003 Blackout in the U.S. and Canada

The August 14, 2003, blackout in the U.S. and Canada is one of the largest blackouts in history. It affected an area with an estimated 50 million people and 61,800MW of power in the states of Ohio, Michigan, Pennsylvania, New York, Vermont, Massachusetts, Connecticut, New Jersey and the Canadian province of Ontario. According to the aftermath report [60], the failure started with a generator failure in Ohio due to an underpredicted reactive load to serve high air conditioning demand. After the initial failure, the Ohio grid operators were forced to import power which caused more line failures due to overloads and lines touching nearby trees. Within hours, the line failures cascaded and caused failure in major tie-lines between ISOs. This resulted in disconnection of the Eastern interconnection into East and West parts which caused further frequency and voltage instabilities and a large-scale blackout. The details of the events leading to the blackout can be found in [60].

How an adversary could have initiated a similar scenario? In a relatively hot summer day (but not the hottest day), an adversary could have initiated the same event by overloading the Ohio system by increasing the reactive power demand by remotely starting several air conditioners. This could cause an unexpected shortage in reactive power generation and possibly the same generator failure and consequent voltage collapse events.

A.2 The 2003 Blackout in Italy

The September 28, 2003, blackout was the most serious blackout in Italy and caused an outage almost everywhere in Italy. At around 3pm in the afternoon, Italy was importing 3,610MW and 2,212MW of power from Switzerland and France, about 600MW and 400MW above their scheduled exchange agreements, respectively. At this time, one of the tie-lines between Switzerland and Italy tripped due to an overload and touching a tree. This resulted in an overload in another tie-line between the two countries and tripping of the second line. After, the second line failure, further lines between Italy and France, Austria, and Slovenia tripped due to overloads and caused the Italian grid to be disconnected from the continental European grid. This resulted in a huge imbalance between supply and demand within Italy and a frequency drop that could not be recovered despite further aggres-

sive load shedding. The details of the events leading to this blackout can be found in [59].

How an adversary could have initiated a similar scenario? An adversary could actively monitor the power flow on the tie-lines through European grids' websites and overload the tie-lines by increasing power demand in Italy and possibly decreasing power demand in Switzerland or France. This could have resulted in the failure of the same tie-lines and subsequent failures.

A.3 The 2011 Blackout in Arizona-Southern California

The September 8, 2011, Arizona-Southern California affected approximately 2.7 million people. It started with a single high voltage line failure due to a fault which redistributed power towards the San Diego area on a hot day during hours of peak demand. Within minutes this redistribution of power resulted in more line and transformer failures (which are modeled as line failures in simulations in the previous section) and eventually separation of the San Diego area from rest of the Western Interconnection. This separation resulted in a huge imbalance between the supply and demand in the San Diego area and a frequency drop which caused generation tripping and a blackout. The details of the events can be found in [9].

How an adversary could have initiated a similar scenario? An adversary could have caused the same initial line failure (which was operating within 78% of its capacity) by increasing the demand in the San Diego area and possibly reducing the demand in Arizona.

A.4 The 2016 Blackout in South Australia

The September 28, 2016, blackout in South Australia affected approximately 1 million customers. Extreme weather conditions on September 28 caused failure in three transmission lines. Following these failures, there was a 456MW reduction in wind generation in the South Australia grid which resulted in an increase in imported power and further tripping of the tie-lines. As a result, the South Australia grid was separated from rest of the Australian grid. This resulted in 900MW imbalance in supply and demand, and a sudden drop in the frequency which caused a blackout in the system. The details of these events can be found in [13].

What is special about this blackout is that a big portion of the electric power in South Australia is generated by wind turbines and solar panels (about 75%) which have very low inertia. This is the main reason for the very quick drop in the frequency after the separation of the South Australian grid from the rest of the interconnection, without the grid operator having a chance to respond to the imbalance by load shedding. This event, in particular, shows that in places or times that renewable resources have a higher share of the power generation, the grid is

much more vulnerable to the MadIoT attacks that cause sudden increases in the demand.

How an adversary could have initiated a similar scenario? Due to the low inertia of the South Australian grid, the sudden increase in the demand by an adversary in the area should be compensated by the tie-lines. This, depending on the amount of the increase, can potentially result in the overload of the tie-lines and their failure. Once they fail and the system is islanded, it may collapse because of the supply and demand imbalance and a quick frequency drop.

B Extra Simulations and Details

In this appendix, we present supplemental simulation results.

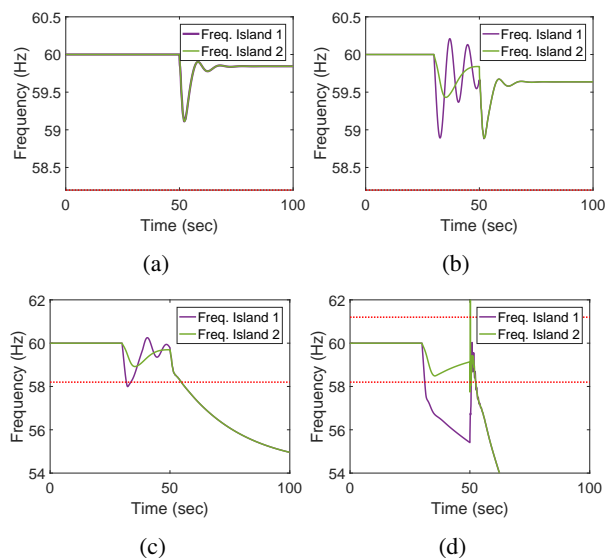


Figure B.1: Frequency disturbances during the black start due to unexpected increases in all the load buses by an adversary (as described in Section 4.2.2), ignoring generators' frequency cut-off limits (shown by red dashed lines). The maximum power outputs for the generators' governors are different in this figure from that of the generators in Fig. 11. (a) Normal black start operation in the absence of an adversary. (b) Demand increases of $10MW$ at the load buses before the reconnection of the two islands. (c) Demand increases of $20MW$ at the load buses before the reconnection of the two islands. (d) Demand increases of $30MW$ at the load buses before the reconnection of the two islands.

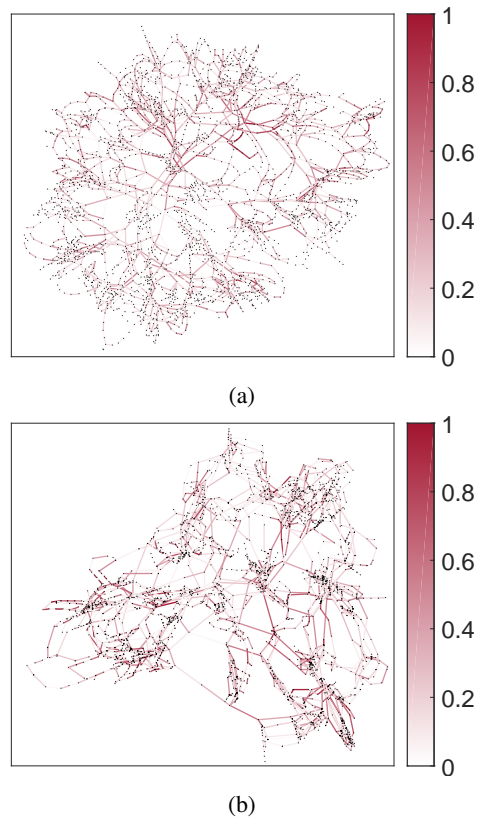


Figure B.2: Polish grid lines' power flow to capacity ratio in (a) Summer 2004 and (b) Summer 2008.

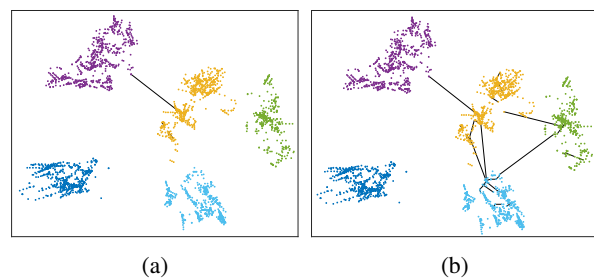


Figure B.3: Tie-line vulnerabilities in the partitioned Polish grid 2008. (a) Failures in the tie-lines between the yellow area and the purple area caused by decreasing the demand by 1% in the former and increasing the demand by 1% in the latter. All the failed lines are shown in black. (b) Failures in several tie-lines caused by decreasing the demand by 1% in the yellow area and increasing the demand by 0.3% in the purple, dark blue, and light blue areas. All the failed lines are shown in black.